REPORT DOCUMENTATION PAGE

Public reporting burden for this collection of information is estimated to average 1 hour per response, including the time for reviewing instructions, searching existing data sources, gathering and maintaining the data needed, and completing and reviewing this collection of information. Send comments regarding this burden estimate or any other aspect of this collection of information, including suggestions for reducing this burden to Department of Defense, Washington Headquarters Services, Directorate for Information Operations and Reports (0704-0188), 1215 Jefferson Davis Highway, Suite 1204, Arlington, VA 22202-4302. Respondents should be aware that notwithstanding any other provision of law, no person shall be subject to any penalty for failing to comply with a collection of information if it does not display a currently valid OMB control number. **PLEASE DO NOT RETURN YOUR FORM TO THE ABOVE ADDRESS.**

1. REPORT DATE *(DD-MM-YYYY)*	2. REPORT TYPE	3. DATES COVERED *(From - To)*
02-28-2012	Final Report	04/15/2009 - 11/30/2011

4. TITLE AND SUBTITLE

Distributed MIMO Radar for Imaging and High Resolution Target Localization

5a. CONTRACT NUMBER

5b. GRANT NUMBER
FA9550-09-1-0303

5c. PROGRAM ELEMENT NUMBER

6. AUTHOR(S)

Alexander M. Haimovich

5d. PROJECT NUMBER

5e. TASK NUMBER

5f. WORK UNIT NUMBER

7. PERFORMING ORGANIZATION NAME(S) AND ADDRESS(ES)

New Jersey Institute of Technology
University Heights
Newark, NJ 07102

8. PERFORMING ORGANIZATION REPORT NUMBER

9. SPONSORING / MONITORING AGENCY NAME(S) AND ADDRESS(ES)

Air Force Office of Scientific Research - Dr. Jon Sjogren

10. SPONSOR/MONITOR'S ACRONYM(S)

AFOSR

11. SPONSOR/MONITOR'S REPORT NUMBER(S)
AFRL-OSR-VA-TR-2012-0532

12. DISTRIBUTION / AVAILABILITY STATEMENT

A

13. SUPPLEMENTARY NOTES

14. ABSTRACT

The research supported by the grant: (a) develops the Cramer-Rao lower bound (CRLB) of the target localization estimation error for the general case of MIMO radar with multiple waveforms with non-coherent and coherent observations; (b) finds a closed-form solution for the best linear unbiased estimator (BLUE) of target localization for coherent and non-coherent MIMO radars, providing a closed-form solution and a comprehensive evaluation of the performance of the estimator's MSE. This gives insight into the relation between sensor locations, target location, and localization accuracy through the use of the geometric dilution of precision (GDOP) metric; (c) present an analysis on the ambiguity arising in the high resolution localization due to sidelobe characteristics of the MIMO system using the Ziv-Zakai Bound (ZZB). (d) leveraging the concept of compressed sensing, it shows that by properly choosing a sufficient number of random sensors the ambiguities can be made arbitrarily small. Furthermore, the number of sensors can be trade with computational complexity, demonstrating that high resolution can be obtained with a relatively low number of randomly placed sensors.

15. SUBJECT TERMS

MIMO radar, High-Resolution radar

16. SECURITY CLASSIFICATION OF:			17. LIMITATION OF ABSTRACT	18. NUMBER OF PAGES	19a. NAME OF RESPONSIBLE PERSON
a. REPORT	b. ABSTRACT	c. THIS PAGE		19	19b. TELEPHONE NUMBER *(include area code)*

Distributed MIMO Radar
for Imaging and High Resolution Target Localization

Alexander M. Haimovich

February 23, 2012

Abstract

The Air Force Office of Scientific Research supported the research on MIMO radar carried out at the New Jersey Institute of Technology during the period from April 2009 to November 2011 under the agreement number FA9550-09-1-0303. The purpose of this report is to summarize the proceedings and findings of the studies supported by this agreement. The report addresses two broad topics: (i) performance bounds for localization, (ii) applications of compressive sensing methods to target localization. Two types of bounds were developed for target localization with MIMO radar: Cramer-Rao bound for high signal to noise ratio (SNR), and Ziv-Zakai bound that effective for a wide range of SNRs. More specifically, the research supported by the grant: (a) develops the Cramer-Rao lower bound (CRLB) of the target localization estimation error for the general case of MIMO radar with multiple waveforms with non-coherent and coherent observations [1]; (b) finds a closed-form solution for the best linear unbiased estimator (BLUE) of target localization for coherent and non-coherent MIMO radars [2], providing a closed-form solution and a comprehensive evaluation of the performance of the estimator's mean square error; (c) presents an analysis on the ambiguity arising in the high resolution localization due to sidelobe characteristics of the MIMO system using the Ziv-Zakai Bound (ZZB) [3]; (d) leverages the concept of compressed sensing to show that by properly choosing a sufficient number of random sensors [4], [5] it is possible to perform highly accurate target localization with far fewer sensors than other localization methods. Furthermore, the number of sensors can be traded-off with computational complexity,demonstrating that high resolution can be obtained with a relatively low number of randomly placed sensors.

1 Introduction

Detection, estimation, and tracking of targets are basic radar functions. Limited data support and low signal-to-noise ratios (SNR) are among the many challenges frequently faced by localization systems. Another challenge is the presence of nearby targets, in terms of location or Doppler, since closely spaced targets are more difficult to discriminate. In multiple input multiple output (MIMO) radar, targets are probed with multiple, simultaneous waveforms. Relying on the orthogonality of the transmitted waveform, returns from the targets are jointly processed by multiple receive antennas. Depending on the mode of operation and system architecture, MIMO radars have been shown to boost target detection, enhance spatial resolution,

and improve interference suppression. MIMO radars achieve these advantages by capitalizing on a larger number of degrees of freedom than "conventional" radar.

A MIMO radar system is defined in general as a radar system employing multiple transmit antennas, and having the ability to jointly process signals reflected by targets and received at multiple antennas. A MIMO radar system may be configured with its antennas collocated [6] or distributed over an area [7, 8]. We refer to radio elements of a MIMO radar as *nodes*. Nodes may be equipped with a transmitter, a receiver or a transceiver. In distributed MIMO radar, the system's antennas are spaced by many wavelengths and may observe a target from different aspects simultaneously. Signals returned from targets can be processed either coherently or non-coherently. Non-coherent processing requires nodes to be time synchronized, while phase synchronization is necessary to enable coherent processing. The coherent/non-coherent nomenclature in this report relates to processing that involves multiple nodes. It is understood that even in the non-coherent regime, all nodes are capable of providing a *local* phase reference, such as needed for Doppler processing. In this report, *coherence* is then the synchronization of phase references of *multiple* nodes.

Non-coherent localization refers to a process that relies on time delays for localization. A distributed MIMO radar architecture offers several important advantages. In a non-coherent regime, *multistatic* observations of a target's radar cross section (RCS) may support a *diversity gain* that averages out RCS scintillations [9]. Also, a distributed topology, implies a larger footprint of the system, leading to improved target localization by multilateration [1]. Finally, observing the target from different directions improves Doppler processing for slow targets and may overcome the problem of blind target velocities [10, 11, 12]. Accuracy and resolution of MIMO radar non-coherent localization are limited by the bandwidth of the transmitted signals. The works funded by this grant propose approaches exploiting the spatial sparsity of targets to attain higher resolution localization than that of classical cross-correlation or superesolution-based approaches.

Coherent localization refers to a process in which distributed nodes can exploit phase information forming a very large effective aperture and leading to very high spatial resolution. In some cases, the high spatial resolution means that a target is constituted of multiple resolution cells. In such cases, coherent MIMO radar can obtain detailed target information through microwave tomography techniques. For example, a classical approach to obtain a microwave image is to cover the area of interest with a grid, and apply a beamformer to focus the array on each of the grid points. The image is formed by registering the strength of the returns as a function of grid point. Localization or imaging by beamforming of large, thinned arrays has high spatial resolution, but also gives rise to high spurious sidelobes [13]. We have propose novel approaches for controlling the sidelobes including exploiting the spatial sparsity of targets and optimizing the transmitted waveforms. This approach is intimately related with the emerging field of *compressive sensing* which has generated tremendous interest in the community. In compressive sensing, one seeks to recover a K-sparse vector $\mathbf{x}$ of length G, $K \ll G$, from a small number $N \ll G$ of linear observations of the form $\mathbf{y} = \mathbf{Ax}$, where the matrix $\mathbf{A}$ is commonly referred to as *dictionary*. In localization, the idea is to recast the inverse problem (i.e., determining the source location from sensors observations) in an optimization framework, where the (known) columns of $\mathbf{A}$ are the steering vectors (array response) for a *grid* of possible source locations, such that the unknown vector $\mathbf{x}$ incorporates information on the location and strength of the sources. While the system $\mathbf{y} = \mathbf{Ax}$ is highly underdetermined, finding conditions that guarantee correct recovery when the unknown vector $\mathbf{x}$ is sparse, has been a main topic of research and one of the underpinnings of compressive sensing theory. In addition to new algorithms, several methods proposed in the past has been reinterpreted, providing links to other fields. Works funded by this grant [4, 5] enforce links between random arrays and compressive sensing algorithms.

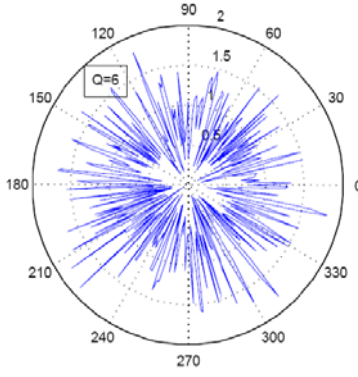### 1.0.1 MIMO radar overview

Figure 1: Monostatic radar cross section of a target consisting of $Q = 6$ isotropic scatterers.

In this section, we introduce the target and signal models for a distributed MIMO radar with M transmitting nodes, N receiving nodes, and an extended target consisting of Q isotropic scatterers with complex amplitudes a_q, $q = 1, ..., Q$. Modeling a complex target as a collection of isotropic scatterers is a classical approach going back to seminal works in radar [14, 15, 16]. Assume that the scatterers are located in a plane that also contains the transmit and receive nodes. The scatterers' locations are denoted by two-dimensional vectors $\mathbf{u}_q$, $q = 1, ..., Q$. Let the transmitting nodes emit waveforms with complex envelopes $s_k(t)$, $k = 1, ..., M$ that modulate a carrier ω_c. Let $\tau_{tk}(\mathbf{u}_q)$ be the time delay from transmission to a scatterer located at $\mathbf{u}_q$ and $\tau_{rl}(\mathbf{u}_q)$ the time delay from the scatterer to receive node l. The signal reflected from the scatterer and received at node l is expressed

$$y_{kl}(t) = h_{kl}(\mathbf{u}_0) s_k [t - (\tau_{tk}(\mathbf{u}_0) + \tau_{rl}(\mathbf{u}_0))], \qquad (1)$$

where $h_{kl}(\mathbf{u}_q) = a(\mathbf{u}_q) e^{-j\omega_c(\tau_{tk}(\mathbf{u}_0)+\tau_{rl}(\mathbf{u}_0))}/r_{kl}(\mathbf{u}_q)$, $h_{kl}(\mathbf{u}_0) = \sum_{q=1}^{Q} h_{kl}(\mathbf{u}_q)$, $r_{kl}(\mathbf{u}_q)$ is the distance along the path transmitter k-location $\mathbf{u}_q$-receiver l, and $\mathbf{u}_0$ is a convenient point representing the whole target, for example the RCS center of gravity. To simplify notation, in this proposal, we will assume that for the applications of interest, the distances $r_{kl}(\mathbf{u}_q)$ are constant for all k, l, and are incorporated in $a(\mathbf{u}_q)$. In summary, the target gains $h_{kl}(\mathbf{u}_0)$ represent the combined effect of an extended target found in the propagation path between transmitter k and receiver l and with an RCS center of gravity at $\mathbf{u}_0$.

The immediate question arises what are the properties of the target gleaned from the coefficients $h_{kl}(\mathbf{u}_0)$. One way to approach this question is to find the relation between the $h_{kl}(\mathbf{u}_0)$'s and the familiar notion of RCS. The RCS is proportional to the power scattered by the target in a certain direction [16]. The familiar *monostatic* RCS is obtained when a single node is used to both transmit and receive. The monostatic RCS is then (up to a constant factor) $\sigma(\mathbf{u}_0) = |h_{11}(\mathbf{u}_0)|^2$. In Fig. 1, is shown an example of a composite target of $Q = 6$ isotropic, equal scatterers. RCS lobes are evident, as they are in the RCS of actual complex targets (e.g., the aircraft RCS plot shown in [16, p. 40]). The terms $|h_{kl}(\mathbf{u}_0)|^2$ for $k \neq l$ represent the *multistatic* RCS of the target, where the illumination and the observed returns from the target are not from the same direction.

Coherent MIMO radar   When the radar system nodes have access to a global phase reference, the system acts as a very large array. Spatial coherency across the system nodes is maintained only for a target with isotropic RCS. In case of an extended target, coherency is obtained for areas of the target sufficiently small to have isotropic properties. The signal model (1) for a single isotropic target at $\mathbf{u}_0$ becomes

$$y_{kl}(t) = a(\mathbf{u}_0) e^{-j\omega_c(\tau_{tk}(\mathbf{u}_0)+\tau_{rl}(\mathbf{u}_0))} \qquad (2)$$

We refer to a MIMO radar system that exploits the relative phase information between nodes as operating in a *coherent regime*.

Non-coherent MIMO radar   When a global phase reference is not available, but a time reference is, we refer to the MIMO radar system in (1) as operating in a *non-coherent regime*.

2   Cramér-Rao lower bound analysis

The research carried out in the context of the grant explored the localization accuracy gain of MIMO radar and tracking performance. A Cramér-Rao lower bound (CRLB) based study of target localization accuracy
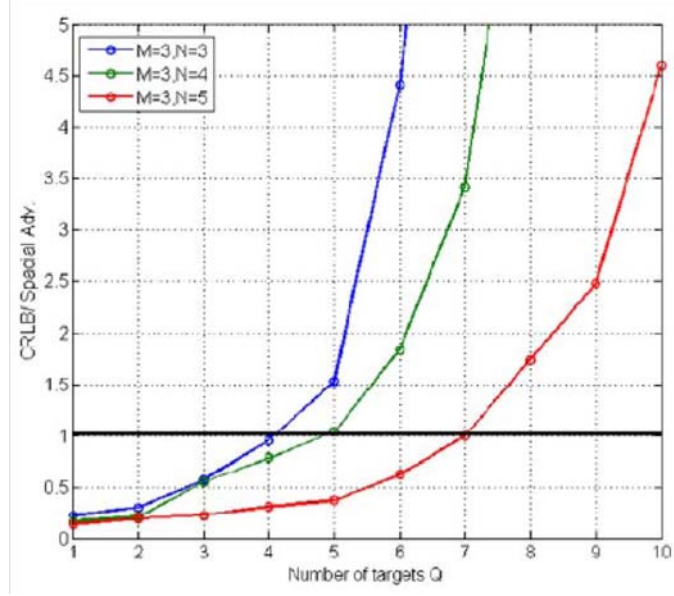
Figure 2: Spatial advantage values for the case of $M = 3$ transmitter and $N = 3$, 4, and 5

performance has demonstrated significant advantage of the widely distributed MIMO radar configuration for both coherent and non-coherent processing. The distinction between non-coherent and coherent applications relies on the need for merely time synchronization between the transmitting and receiving radars vs. the need for phase synchronization. The MIMO radar architecture with coherent processing exploits knowledge of the phase differences measured at the receive antennas to produce a high accuracy target location estimate. In traditional radar systems, bandwidth plays an important role in providing resolution range, i.e. it is inversely proportional to the signal efficient bandwidth.

The research supported by this grant provides an in depth analytical analysis of the localization accuracy gain attainable with the MIMO radar systems. This year of the project, the supported research was particularly extended as to the study of MIMO radar coherent processing gain for the multiple target case, performance sensitivity to phase synchronization errors and tracking capabilities of MIMO radar systems with non-coherent processing.

The CRLB of the target localization estimation error is developed for the general case of MIMO radar with multiple waveforms with non-coherent and coherent observations. The analytical expressions of the CRLB are derived for the case of orthogonal waveforms [1]. It is shown that the CRLB expressions, for both the non-coherent and coherent cases, can be factored into two terms: a term incorporating the effect of bandwidth, carrier frequency and SNR, and another term accounting for the effect of sensor placement, defined as spatial advantage. The CRLB of the standard deviation of the localization estimate with non-coherent observations is shown to be inversely proportional to the signals averaged effective bandwidth. Dramatically higher accuracy can be obtained from processing coherent observations. In this case, the CRLB is inversely proportional to the carrier frequency. This gain is due to the exploitation of phase information, and is referred to as coherency advantage.

Formulating a convex optimization problem, it is shown that symmetric deployment of transmitting and receiving sensors around a target is optimal with respect to minimizing the trace of the CRLB. The closed-form solution of the optimization problem also reveals that optimally placed M transmitters and N receivers reduce the CRLB on the variance of the estimate by a factor $MN/2$ (in [1]). A closed-form solution is developed for the best linear unbiased estimator (BLUE) of target localization for coherent and non-coherent
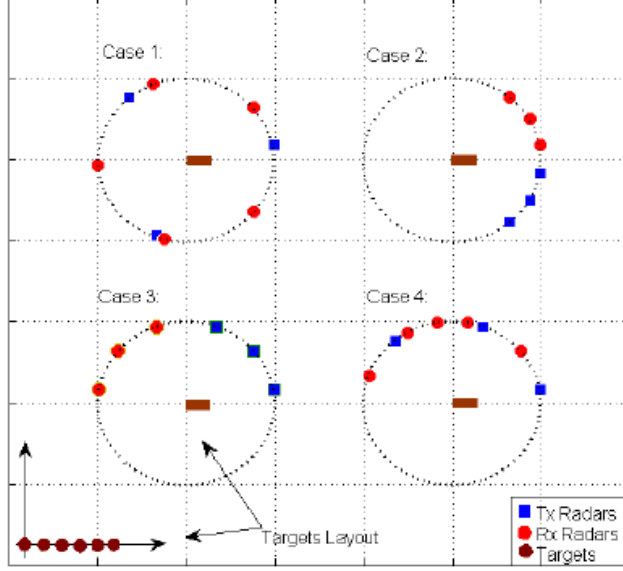
4

Figure 3: System layout for cases 1 to 4.

MIMO radars [2]. It provides a closed-form solution and a comprehensive evaluation of the performance of the estimator's MSE. This estimator provides insight into the relation between sensor locations, target location, and localization accuracy through the use of the GDOP metric. This metric is shown to represent the spatial advantage of the system. Contour maps of the GDOP, provide a clear understanding of the mutual relation between a given deployment of sensors and the achievable accuracy at various target locations. An evaluation of target localization performances for MIMO radar with coherent processing and single-input multiple-output (SIMO) radar systems, based on the BLUE, is provided in [20]. The best achievable accuracy for both configurations is derived. MIMO radar systems with coherent processing are shown to benefit from higher spatial advantage, compared with SIMO systems. The advantage of the MIMO radar scheme over SIMO is evident when considering the achievable accuracy for a radar system with M transmitters and N receivers, rather than 1 transmitter and MN receivers. It is shown that MIMO radar, with a total of $M + N$ sensors, has twice the performance (in terms of localization MSE) of a system with $(MN + 1)$ sensors [20].

The localization performance study is extended to the case of multiple targets, with coherent processing [21]. The CRLB for the multiple targets localization problem is derived and analyzed. The localization is shown to benefit from coherency advantage. The trade-off between target localization accuracy and the number of targets that can be localized is shown to be incorporated in the spatial advantage term. An increase in the number of targets to be localized exposes the system to increased mutual interferences. This trade-off depends on the geometric footprint of both the sensors and the targets, and the relative positions of the two. Numerical analysis of some special cases offers an insight to the mutual relation between a given deployment of radars and targets and the spatial advantage it presents. In Figure 2 the spatial advantage value is drawn for the case of $M = 3$ transmit antennas employed with $N = 3$, 4, and 5 receive antennas. Both transmit and receive antennas are located with angular spacing of $2\pi/M$ and $2\pi/N$ with respect the axis origin. Targets are located in a linear array with the first target located at $(0,0)$ and the rest located at $(x_q = x_q - 1 + 10, y_q = 0)$. At $Q = 1$, the resulting spatial advantage in Figure 2 follow the results for a single target where the values of $2/9$, $2/12$, and $2/15$ are obtained. It is observed that an increase in the number of targets results in a decrease in the spatial advantage and therefore, in
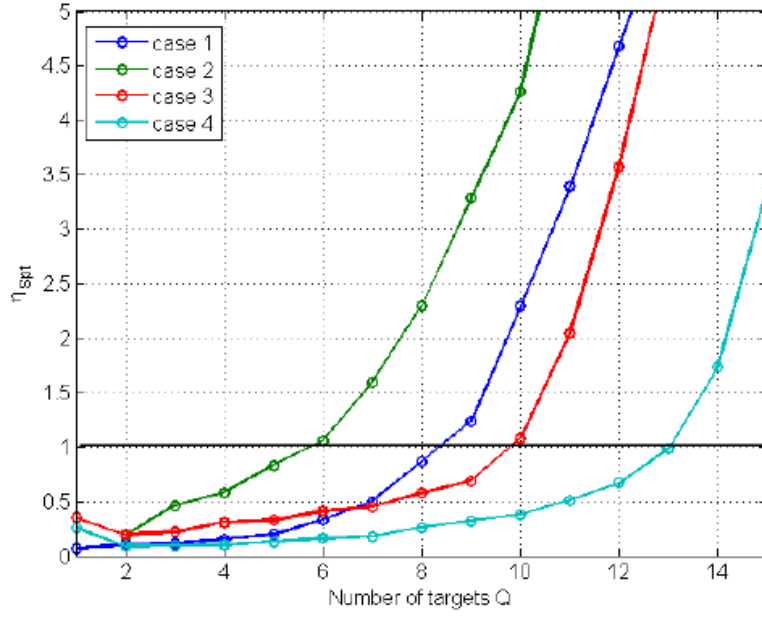
5

Figure 4: Spatial advantage values for cases 1 to 4.

$$\Delta \approx (0, 0.01, 0.02, 0.04, 0.09, 0.18, 0.36, 0.7) \cdot \pi$$

$$\sigma_{\Delta}^2 = (0, 0.00012, 0.0005, 0.002, 0.008, 0.03, 0.125, 0.5) \cdot \pi^2$$
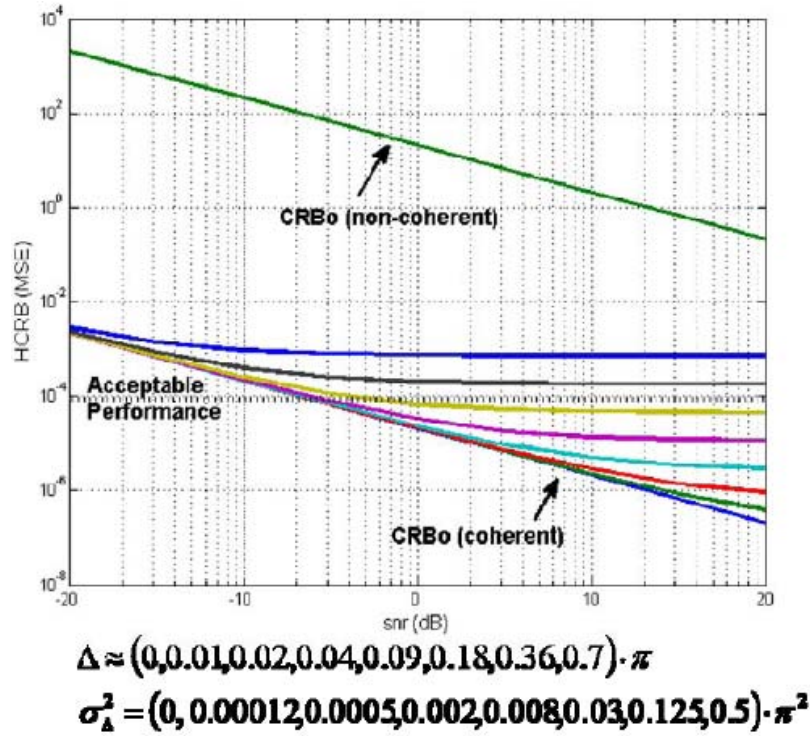
Figure 5: HCRB for a 4x5 MIMO radar system and different phase synchronization errors.

the accuracy. This decrease may be moderated by increasing the number of transmit and receive radars, MN. In the case of $M = N = 3$ three targets enjoy spatial advantage while with $M = 3$ and $N = 5$ six targets still benefit from spatial advantage. For the latter case, up to four targets are located with high accuracy. To identify favorable radars locations with respect to the targets layout, four special cases, demonstrated in Figure 3, are analyzed. The averaged value of the spatial advantage versus the number of targets is drawn in Figure 4. It is observed in the figure that a symmetrical placement, as shown in Case 1, is not an optimal one. Rearranging the radars, in the more favorable setting (as in Case 4) demonstrates a performance gain, in terms of the number of targets and the spatial advantage, achieved without any change in the number of antennas. This is a result of the larger transmit/receive aperture sets contributing to larger delays. Placing the radars in a broadside horizontal spread (as in Case 3) provides better spatial advantage and moderate performance loss rate when compared with Case 2, where a vertical radar setting is used. Increasing the number of radars, as can be noticed from comparing Case 3 and Case 4, allows for localization of more targets with higher spatial advantage and restrained performance loss rate. Improvement in target parameter estimation capabilities is among the advantage of MIMO radar systems [1], in particular, target localization with coherent MIMO radar systems. This performance gain comes with the challenge of attaining phase synchronization in a distributed system. Errors introduced to the system parameters by phase synchronization mismatch, will result in parameter estimation mean-square error (MSE) degradation and bias. The hybrid CRB (HCRB) is used to test the sensitivity of the target localization MSE to phase errors. The HCRB takes into account deterministic unknown parameters, such as the target location, as well as random parameters, phase calibration errors, in this case. This bound is derived for coherent MIMO radars, with phase synchronization errors. The effect of the number of radars, their geometric layout, and the phase mismatch MSE is incorporated in the HCRB terms. Synchronization errors are modeled as being random and Gaussian. The closed-form expression for the hybrid CRB is derived for the case of orthogonal waveforms. The bound on the target localization MSE is expressed as the sum of two terms – the first represents the CRB with no phase mismatch, and the second captures the mismatch effect. The latter is shown to depend on the phase error variance, the number of mismatched transmitting and receiving sensors and the system's geometry. For a given phase synchronization error variance, this expression offers the means to analyze the achievable localization accuracy. Alternatively, for a predetermined localization MSE target value, the derived expression may be used to determine the necessary phase synchronization level in the distributed system. The HCRB is evaluated using numerical analysis in Figure 5, with different phase error variances. As phase synchronization over distributed platform is a complex operation and phase errors are unavoidable, the HCRB offers valuable information at the system design level. For a given phase error MSE, the HCRB may be used to derive the attainable target localization accuracy. Otherwise, for a given system performance goal on localization accuracy, the HCRB provides with an upper bound on the necessary phase error MSE values.

3 Ziv-Zakai Lower Bound analysis

Localization has been intensively studied and broadly applied in many fields including radar, sonar, seismic analysis, and sensor networks. Due to the many applications, each characterized by its own set of requirements, the localization problem remains an active subject of research. The main figure of merit for the localization problem is accuracy. In previous work on localization of targets in MIMO radar systems, we have shown the potential for significant gains when localization processing exploits the phase information among pairs of radars. Localization systems that exploit the phase information are referred to as coherent, in contrast to noncoherent systems, which exploit envelope measurements. Evaluation of the CRLB reported on in 2009 has shown that at high SNR, the accuracy of coherent MIMO radar systems is of the order of the carrier wavelength of the transmitted waveforms. MIMO radar systems with widely distributed elements
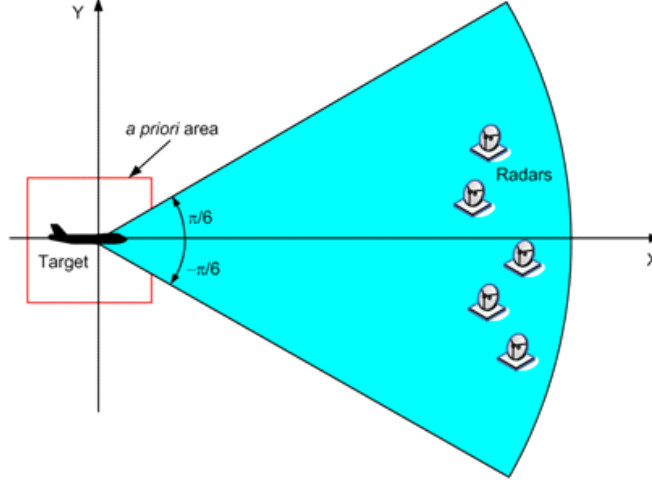
Figure 6: Setup configuration of the MIMO radar system with antennas distributed in a sector.

have high accuracy capabilities of localizing targets, but are also subject to high peak sidelobes in the coherent localization metric. At sufficiently high SNRs, these sidelobes have little impact on performance. Below a threshold SNR however, performance degrades rather quickly. One of the goals of this year's work, was to improve the understanding of the effect of sidelobes on MIMO radar performance and develop ways to predict the performance of localization techniques as a function of SNR and of system parameters. The performance of target localization can be studied through a lower bound on the mean square error (MSE) of the localization estimates. For high SNR, the estimated parameter is affected by noise errors that are too small to cast the estimate outside the main lobe of the localization metric. In this region, the mean square error (MSE) of the estimate is inverse proportional to the Fisher information, and thus performance can be predicted by calculating the CRLB. At low SNR however, due to the effect of sidelobes, performance is affected by large errors, and the CRLB cannot predict performance anymore. In this region, performance can be lower bounded by the Ziv-Zakai Bound (ZZB).

A full theoretical analysis is given in [3]. Here, we present some numerical examples. For these examples, the target was positioned in the center of the coordinate system. The transmitting and receiving radars were distributed randomly in a sector with center at the origin of the axes $(0, 0)$ and with a central angle of radians. The ZZB was computed numerically by averaging over 30 random setups (different radar configurations). The setup is shown in Figure 6. The duration of the observation T was taken such that $BT = 625$ samples, where B is the bandwidth in Hz.In Fig. 7, the ZZB obtained by numerical integration is plotted versus the average SNR, for a 2×4 MIMO configuration (2 transmit and 4 receive antennas), and transmitted signals with bandwidth $B = 200$ kHz and carrier $f_c = 1$ GHz. The CRLB of the target location is also plotted for reference. The a priori interval for the coordinates of the source is set to a square with a side equal to 1 km. From the figure it can be observed that the ZZB versus SNR can be divided into three regions. For low SNR, the ZZB reaches a plateau equal to the standard deviation of the a priori pdf of the source location. In this region performance is dominated by noise, hence the localization error is limited only by the a priori information. For high SNR, the ZZB merges with the CRLB, indicating that the noise errors are too small to cast the estimate outside the mainlobe of the localization metric. This region is the ambiguity free region. Between the two SNR extremes, is the ambiguity region, in which the location estimator is affected by ambiguities created by sidelobes of the localization metric.

In Fig. 8, the ZZB of the error in estimating the abscissa of the source is presented for different carrier frequencies. The results presented in the figure were obtained for a 2×4 MIMO system and $B = 200$
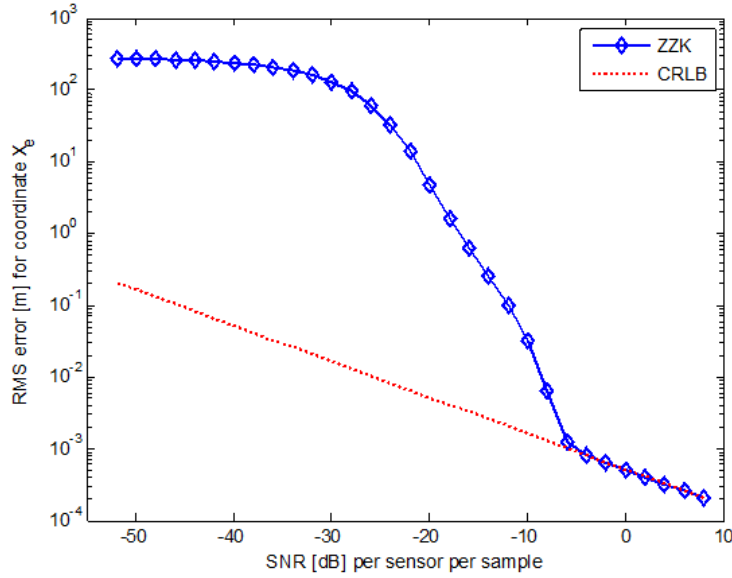
Figure 7: Comparison between different lower bounds: CRLB (red dotted line) and ZZK (blue line with diamonds)

kHz signal bandwidth. The a priori interval for the abscissa of the narrowband source was set to $[-500$ m, 500 m] around the real abscissa. One can observe that if the SNR is high enough, localization accuracy improves with the carrier frequency. In the ambiguity region, the performance degrades with increasing carrier frequency. This result is explained by the increase in sidelobes with the carrier frequency. The effect of sidelobes in the localization metric can be reduced by increasing the number of sensors. This is illustrated in Figure 9. The effect of bandwidth on localization is shown in Figure 9. An increase in bandwidth leads to a reduction in the sidelobes, leading to smaller errors in the ambiguity region. This is due to the fact that the transmitted pulse autocorrelation function serves as the envelope of the localization metric. This envelope, which becomes narrower with the increase in bandwidth, forces the sidelobes to decay faster.

3.1 Target Tracking with MIMO Radar

In this work [18], we studied moving target tracking performance in MIMO radar systems with distributed antennas and non-coherent processing. Due to the use of multiple, widely distributed antennas, MIMO radar architectures support both centralized and decentralized tracking techniques. Each receiving radar may contribute to central processing by providing either raw data or partially/fully processed data. Estimation performance of centralized and decentralized tracking is analyzed through the Bayesian Cramér-Rao bound (BCRB). The BCRB offers insight into the effect of the radars geometric layout, the target location, and propagation path losses on tracking accuracies. It was shown that, with different propagation path loss, the manner in which decentralized estimations are combined in the fusion center effects the overall estimation performance. Two tracking algorithms were proposed, corresponding to respectively, a centralized and decentralized modes of operation. It is demonstrated that communication requirements and processing load may be reduced at a relatively low performance cost. Based on mission needs, the system may use either approach: centralized for high accuracy or decentralized for resource-aware tracking.
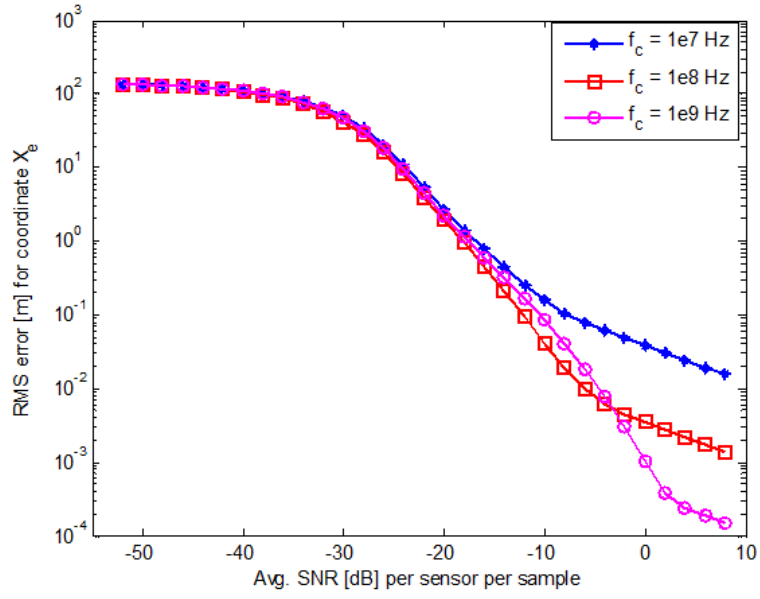
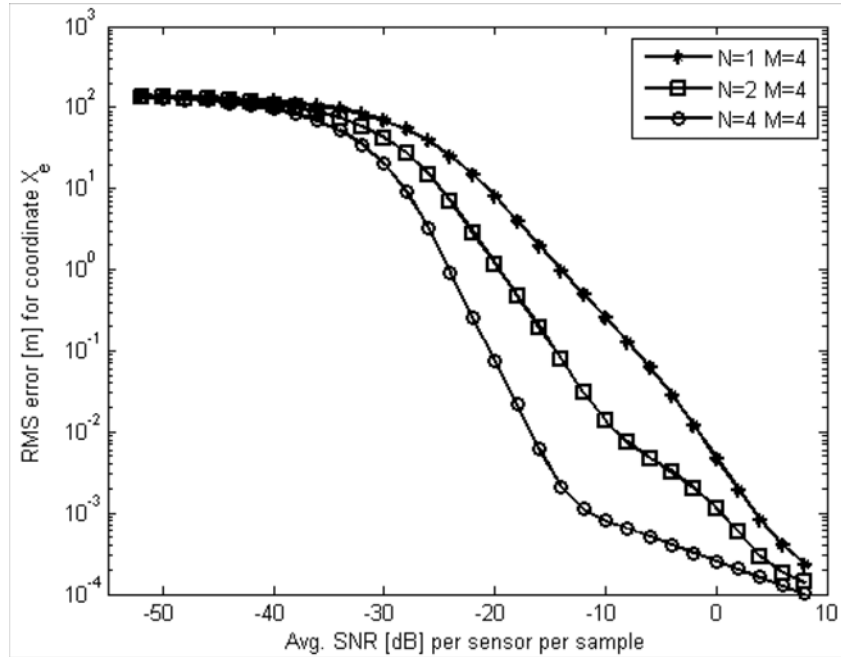Figure 8: Localization accuracy improves with the carrier frequency at high SNR

Figure 9: $B = 200$ kHz, $f_c = 1$ GHz, and coordinates x_e and y_e are uniformly distributed between $[-500$ m; 500 m]
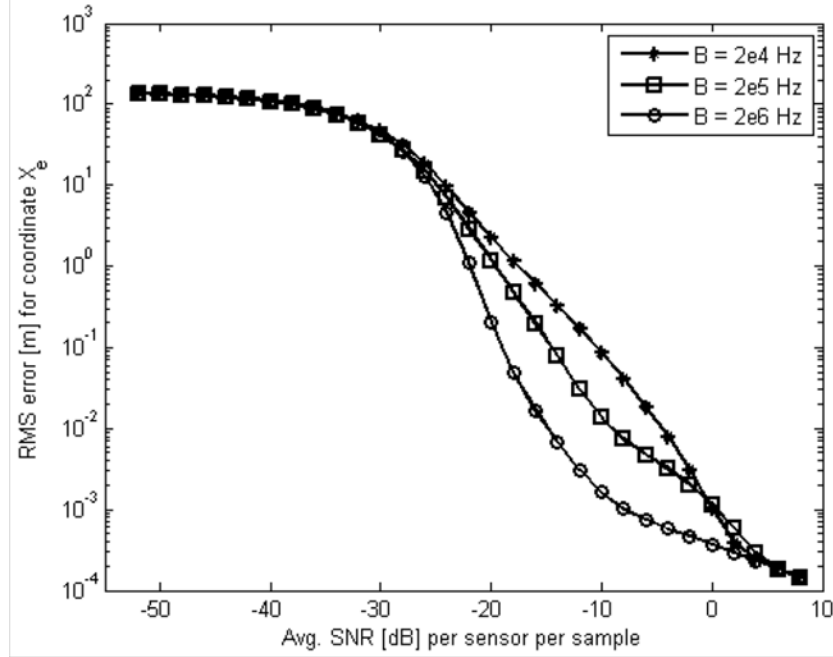
Figure 10: MIMO 2×4 antennas, $f_c = 1$ GHz, and coordinates x_e and y_e are uniformly distributed between $[-500$ m; 500 m$]$

3.2 Effect of Synchronization Errors

Localization advantages of coherent MIMO radar systems rely on full phase synchronization among all participating radars. Phase synchronization errors are practically inevitable, reflecting on the system localization performance. In work reported in [19], quantitative tools were developed to assess the effect of synchronization errors. The lower bound on the mean-square error (MSE) is set by the Hybrid Cramér-Rao bound (HCRB) for the joint estimation of the target location and the phase synchronization offsets at the radars. The latter are modeled as random unknown. The HCRB of the unknown target location was shown to be equal to the CRB derived by discarding the random phase synchronization errors through marginalization, i.e., treating them as nuisance parameters. Therefore, the HCRB closed-form expression provides an asymptotically tight bound on target location estimation MSE at high signal-to-noise ratio (SNR). The bound is shown to follow the CRB in the absence of phase errors up to a threshold point, determined by the synchronization error variance, the SNR, and the number of mismatched transmitting and receiving sensors. Beyond this point, the HCRB asymptotically reaches a lower limit, proportional to the synchronization errors variance and independent of the SNR. The value of the threshold point and lower limit are determined for symmetrical radar deployments.

4 Sparse framework for Localization

Another research area carried out in the context of the grant explored the application of MIMO radar to the estimation of direction-of-arrival (DOA) using a sparse, random array architecture in which a low number of transmit/receive elements are placed at random over a large aperture.

It is well known in array signal processing [22] that resolution improves with the array aperture. A non-ambiguous uniform linear array (ULA) must have its elements spaced at intervals no larger than $\lambda/2$.

For a MIMO radar, unambiguous direction finding of targets is possible for $\lambda/2$-spaced receive elements and $N\lambda/2$-spaced transmit elements (a virtual filled array), where N is the number of receive elements. In compressive sensing parlance, the $\lambda/2$-spaced array and the MIMO virtual filled array perform spatial sampling at Nyquist rate. In this work, we are interested in a random array setup in which the spatial sampling is at sub-Nyquist rates. Recovering targets from undersampled array data, links random arrays to the compressive sensing paradigm (see [4] and references therein).Recently, the signal processing community has seen a paradigmatic shift towards optimization in a sparse framework. One aspect of this new approach is the notion of *compressed sensing*, which enables to capture compressible signals at sampling rates below Nyquist. Consider a discrete signal $\mathbf{x}$ of length L. We say that it is K-*sparse* if at most $K \ll L$ of its coefficients are nonzero (perhaps under some appropriate change of basis). With this point of view, the true information content of $\mathbf{x}$ lives in at most K dimensions rather than L. An example of such a signal pertinent to our work is where $\mathbf{x}$ is constituted of a grid of possible target locations, but only a few targets are present, i.e., only a few of $\mathbf{x}$'s components are non-zero. In terms of signal observations, it makes sense that one should have to measure the signal only $N \simeq K$ times instead of L. This is accomplished by expressing N non-adaptive, linear observations in the form of $\mathbf{y} = \mathbf{A}\mathbf{x}$, where $\mathbf{A}$ is a redundant *dictionary* of size $N \times L$, with $N \ll L$. The matrix $\mathbf{A}$ comprises of information about the channels between the components of signal $\mathbf{x}$ and the observations $\mathbf{y}$. The optimization problem in a sparse framework is to recover $\mathbf{x}$ given the observations $\mathbf{y}$, the matrix $\mathbf{A}$, and the assumption that $\mathbf{x}$ is sparse.

Whereas compressive sensing literature originated in the Single Measurement Vector (SMV) scenario, i.e., $\mathbf{y} = \mathbf{A}\mathbf{x}$, array signal processing is set mainly in the Multiple Measurements Vector (MMV) framework, i.e., $\mathbf{Y} = \mathbf{A}\mathbf{X}$. The compressive sensing approach aims to solve the non-convex combinatorial ℓ_0-norm problem (i.e., $\min \|\mathbf{X}\|_0$ subject to $\|\mathbf{Y} - \mathbf{A}\mathbf{X}\|_F^2 \leq \epsilon$), which can be related to the well known Deterministic Maximum Likelihood (DML) estimator [23]. Both estimators require a multi-dimensional search, infeasible in practical scenarios. The main insight of compressive sensing has been to derive conditions guaranteeing a correct global solution via polynomial complexity (e.g., by solving a convex relaxation of the original problem). These conditions link properties of $\mathbf{X}$ (specifically, the number of active rows/targets K and their linear dependency) with properties of the matrix $\mathbf{A}$ (the smallest number of linearly dependent columns or $\mathrm{spark}\,(\mathbf{A})$). For a matrix $\mathbf{A}$ with MN rows, it trivially holds that $\mathrm{spark}\,(\mathbf{A}) \leq MN + 1$. Assuming this bound is achieved with equality, a necessary and sufficient lower bound on MN for identifiability of the localization problem is $MN > 2K - \mathrm{rank}\,(\mathbf{Y})$ [24]. It is well known in array processing that so-called "super-resolution" techniques, e.g., subspace methods such as MUSIC and ESPRIT are able to attain this bound with equality in a noiseless setting, when the received signal has a full-rank covariance matrix ($\mathrm{rank}\,(\mathbf{Y}) = K$). This is a consequence of the fact that subspace methods are "large sample" realizations of the maximum likelihood estimator for $MN > K$ and uncorrelated signals [23].

In the work supported by the grant [4, 5] we uncover relations between compressed sensing DOA estimation and the number of sensors that are necessary for the estimation errors to be local, i.e., such that a local bound like Cramér-Rao applies. In details we made the following specific contributions: (1) develop a tree-based algorithm, dubbed Multi-Branch Matching Pursuit (MBMP), for the multiple pulse (MMV) setting, typical to radar; establish a lower bound on the number of elements of a random array MIMO radar system for a single measurement vector (SMV) of sub-Nyquist spatial samples when employ the MBMP algorithm.

The main result in [5] is a lower bound on the number of MIMO radar elements required to guarantee successful target estimation with probability greater than $1 - \gamma$:

$$MN \geq K \ln \frac{n}{d_1 \gamma} \qquad (3)$$

where K is the number of targets, n is the number of sidelobes, approximately two times the "virtual array" aperture, and d_1 is proportional to the algorithm complexity. This highlights that it is possible to trade-off
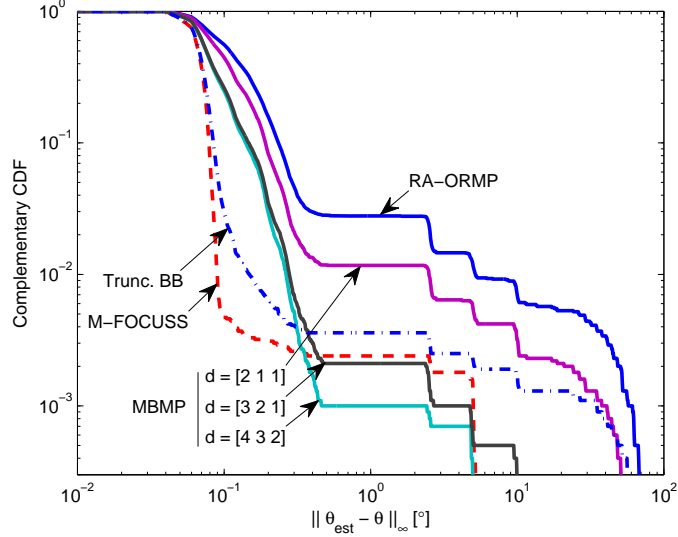
Figure 11: CCDFs of the MBMP algorithm with different tree's spans. Noiseless SMV setting.

sensors for computational complexity.

For the sake of completeness, here we provide some results from the works supported by the grant. As a measure of estimation accuracy, for each realization, we collect the *largest modulo* of the targets' estimation error, i.e., $\left\| \hat{\boldsymbol{\theta}} - \boldsymbol{\theta} \right\|_\infty \triangleq \max_k \left| \hat{\theta}_k - \theta_k \right|$. We then plot the complementary cumulative distribution function (CCDF), defined as $C(x) \triangleq \Pr(X \geq x) = 1 - F(x)$, where F is the cumulative distribution function. The function C is the probability of having an error *greater* then the abscissa, such that a good technique shifts the CCDF towards the bottom-left of the figure. This choice highlights both the resolution and the probability of ambiguities (sidelobes' detections). We analyze first the behavior of the proposed MBMP algorithm in a noiseless SMV setting. Fig. 11 plots the CCDFs of the recovery error for a variety of tree spans of the MBMP algorithm (i.e., different branch vectors $\mathbf{d}$), and compares it with the performance of certain compressive sensing techniques, as well as with the Truncated BB algorithm proposed in [4] truncated at 100 iterations. The system settings are $M = N = 5$ elements, noiseless $\sigma^2 = 0$, and $K = 3$ targets at $\boldsymbol{\theta} = [-5°, 0°, 5°]$. It can be seen how the probability of errors greater then $0.6°$ (i.e., the random array resolution) diminishes as the tree's span is increased. Moreover, the proposed MBMP algorithm outperforms the Truncated BB with less then half of the latter complexity (i.e., from the discussion of computational complexity, for $\mathbf{d} = [4, 3, 2]$, we have $D = 40$). This favorable outcome stems from the rules used to build the algorithm's tree.

Next, we focus on a scenario with high noise and multiple pulses (MMV). The system settings are $M = N = 5$, $P = 200$, $\sigma^2 = 1$, and $K = 4$ targets at $\boldsymbol{\theta} = [-7.5°, -2.5°, 2.5°, 7.5°]$. Fig. 12 plots the CCDFs of the recovery error for various versions of the MBMP algorithm (i.e., for different branch vector $\mathbf{d}$), and compares it with the performance of compressive sensing techniques and with the MUSIC estimator. The main difference from the noiseless SMV scenario is that M-FOCUSS is now performing much worse than MBMP. It is well known that for a large sample (high P) the estimated covariance matrix becomes accurate. Subspace methods exploits that through the separation of signal and noise subspaces. This gain is not exploited by the M-FOCUSS algorithm, resulting in poorer performance. Nonetheless, MUSIC (a subspace method) does not perform that well either. Now, this can be explained by the non-iterative decision strategy of the algorithm: the K targets are estimated *simultaneously* as the K highest peaks of the MUSIC spectrum. In contrast, MBMP refines its estimates iteratively based on a successive-
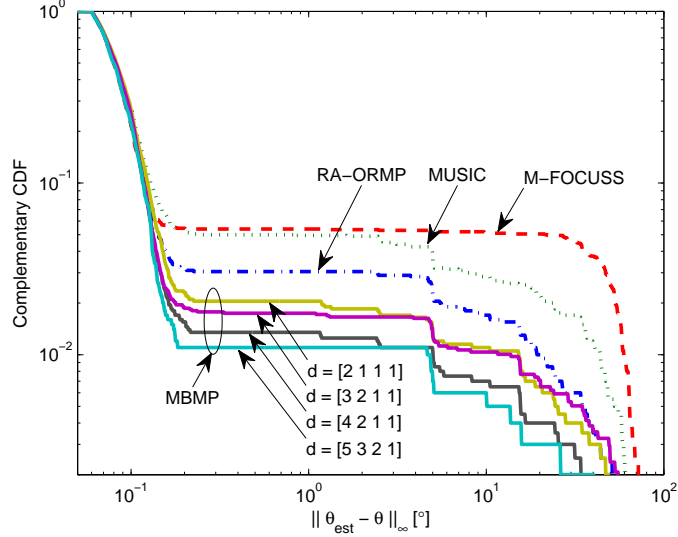
Figure 12: CCDFs of the MBMP algorithm with different tree's spans. Noisy MMV setting.

decision strategy (following the tree's levels). As a result, this strategy enables to reduce the errors without compromising the computational complexity.

In the next experiment, we investigate the resolution capabilities with respect to SNR and sample support. We are asking how high must SNR be to deliver "super-resolution" (i.e., resolve targets less then one beamwidth apart)? We compare a MIMO random array architecture and a "virtual ULA" configuration. The system settings are $M = N = 3$ sensors and $K = 3$ targets at $\boldsymbol{\theta} = [-5°, 0°, 5°]$. The random array has a virtual aperture of 14λ (resulting in a beamwidth of $\approx 4°$), while the "virtual ULA" has an aperture of 4λ (beamwidth of $\approx 14°$). The number of sensors and the array aperture have been selected such that the random array beamwidth is less then the minimum target separation $\Delta\theta = 5°$, while the "virtual ULA" beamwidth is greater then $\Delta\theta$. Once again, this is to investigate how an ambiguous but large aperture MIMO random array compares with an ambiguity-free "virtual ULA" where resolution is constrained to the array aperture. In a noiseless scenario, we expect super-resolution methods to recover all the targets with probability 1, irrespective of "virtual ULA" aperture. Fig. 13 plots the probability of having a recovery error greater then $1°$ varying the noise level and for different number of pulses ($P = 5, 10$ and 50). The MBMP algorithm ($\mathbf{d} = [5, 3, 2, 1]$) is employed in the MIMO random array and in the "virtual ULA" setting. In the latter, the ESPRIT algorithm is shown for comparison. The superiority of the random array, which has higher array resolution, is evident. Moreover, the proposed algorithm is found to be more robust then ESPRIT to limited data support.

5   Conclusions

In this report, we overview the concepts of MIMO radar and reviewed some recent work focusing on applications with distributed MIMO Radar for imaging and high resolution target localization. Generally speaking, MIMO radars transmit multiple waveforms, receive signals at multiple antennas, and process them jointly. Processing may be carried out non-coherently or coherently (as detailed above). The main topics discussed in the paper can be summarized as follows:

- An analytical expressions for the estimation errors of coherent and noncoherent MIMO radar using the CRLB was developed. Results shown that when the processing is coherent and the phase is processed,
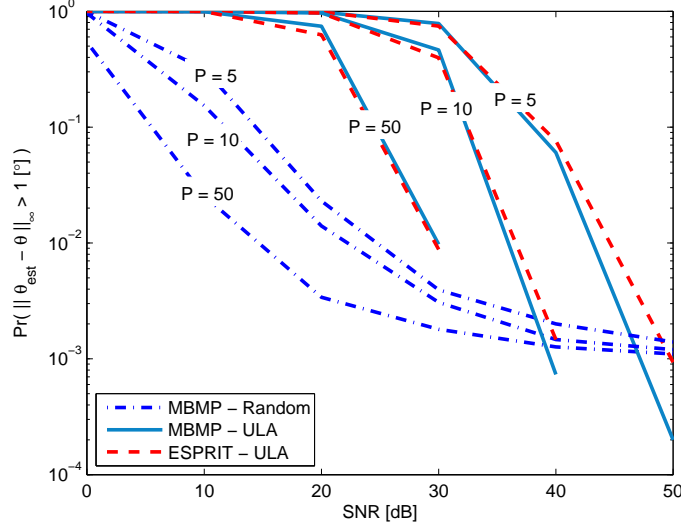
14

Figure 13: Sidelobe error probability for random array and ULA with the MBMP and ESPRIT algorithms.

there is a reduction in the CRLB values (standard deviation of the estimates) by a factor of over the case when the observations are noncoherent. We referred to this gain as coherency gain.

- The Ziv-Zakai bound for vector parameters was used to derive a lower bound on the MSE of estimating the location of a target with a MIMO radar system. The bound is a convenient tool for analyzing the localization performance for different parameters such as carrier frequency, signal bandwidth, and number of sensors.

- The source localization problem in MIMO radar is recast in a sparse representation framework. We develop a global search algorithm for the sparse recovery problem, and derive an explicit lower bound on the number of random array elements needed to achieve a prescribed probability of correct DOA estimation. The lower bound provides specific insight into links between random arrays and compressive sensing algorithms, and demonstrates that a high resolution can be obtained with a relatively low number of randomly placed sensors.

Distributed MIMO Radar is a very promising concept for high performance radars. While localization by coherent MIMO radar provides significantly better performance than noncoherent processing, it faces the challenge of multisite systems phase synchronizing, and needs to deal with the ambiguities stemming from the large separation between sensors. Moreover, among the engineering challenges there are centralized coordination of sensor transmissions, synchronized communication with a processing center, and highly precise phase synchronization among sensors (of the order of nanoseconds for resolutions in meters). Research challenges include a better understanding of bistatic and multistatic RCS phenomena, tracking targets with MIMO radar, MIMO radar on airborne platforms, and others.

6   Personnel supported

- Faculty: Alexander M. Haimovich (PI)

- Graduate Research Assistant: Hana Godrich, Vlad M. Chiriac, Marco Rossi.

15

References

[1] Godrich, H.; Haimovich, A.M.; Blum, R.S.; , "Target Localization Accuracy Gain in MIMO Radar-Based Systems," Information Theory, IEEE Transactions on , vol.56, no.6, pp.2783-2803, June 2010.

[2] H. Godrich, A. M. Haimovich, and R. S. Blum, "Target localisation techniques and tools for multiple-input multiple-output radar," in IET Radar, Sonar and Navigation, Vol.3, August 2009, pp. 314 - 327.

[3] V. M. Chiriac and A. M. Haimovich, "Ziv-Zakai lower bound on target localization estimation in MIMO radar systems," Radar Conference, 2010 IEEE , vol., no., pp.678-683, 10-14 May 2010.

[4] M. Rossi, A. M. Haimovich, and Y. C. Eldar, "Global Methods for Compressive Sensing in MIMO Radar with Distributed Sensors," in Proc. Asilomar Conference on Signals, Systems and Computers, Pacific Grove, CA, Nov. 6-9, 2011.

[5] M. Rossi, A. M. Haimovich and Y. C. Eldar, "Spatial Compressive Sensing in MIMO Radar with Random Arrays," to appear in Proc. CISS 2012, Princeton, NJ, Mar. 21-23, 2012.

[6] J. Li, and P. Stoica, "MIMO Radar with Colocated Antennas: Reviewing Recent Work," *IEEE Sig. Proc. Magazine*, September 2007, pp. 106-114.

[7] E. Fishler, A. Haimovich, R. Blum, L. Cimini, D. Chizhik, and R. Valenzuela, "MIMO radar: An idea whose time has come," in *Proc. of the 2004 IEEE Int. Conf. on Radar*, April 2004, pp. 71-78.

[8] A. Haimovich, R. Blum, and L. Cimini, "MIMO Radar with Widely Separated Antennas: Reviewing Recent Work," *IEEE Sig. Proc. Magazine*, January 2008, pp. 116-129.

[9] E. Fishler, A. Haimovich, R. Blum, L. Cimini, D. Chizhik, and R. Valenzuela, "Spatial diversity in radars - models and detection performance," *IEEE Trans. on Sig. Proc.*, vol. 54, March 2006, pp. 823-838.

[10] He, Qian; Lehmann, Nikolaus H.; Blum, Rick S.; Haimovich, Alexander M.; , "MIMO Radar Moving Target Detection in Homogeneous Clutter," Aerospace and Electronic Systems, IEEE Transactions on , vol.46, no.3, pp.1290-1301, July 2010.

[11] Qian He; Blum, R.S.; Godrich, H.; Haimovich, A.M.; , "Target Velocity Estimation and Antenna Placement for MIMO Radar With Widely Separated Antennas," Selected Topics in Signal Processing, IEEE Journal of , vol.4, no.1, pp.79-100, Feb. 2010.

[12] Qian He; Blum, R.S.; Haimovich, A.M.; , "Noncoherent MIMO Radar for Location and Velocity Estimation: More Antennas Means Better Performance," Signal Processing, IEEE Transactions on , vol.58, no.7, pp.3661-3680, July 2010.

[13] Haleem, M.A.; Haimovich, A.; Blum, R.; , "Sidelobe mitigation in MIMO radar with multiple subcarriers," Radar Conference, 2009 IEEE , vol., no., pp.1-6, 4-8 May 2009.

[14] Delano, R.H., "A Theory of target glint or angular scintillation in radar tracking," Proceedings of the IRE , vol.41, no.12, pp.1778-1784, Dec. 1953.

[15] P. Swerling, "Probability of detection for fluctuating targets," *IEEE Trans. on Information Theory*, vol. 6, pp. 269- 308, April 1960.

[16] M.I. Skolnik, *Inotrduction to Radar Systems*, 2nd edition, McGraw-Hill, 1980.

[17] Godrich, H.; Haimovich, A.M.; Blum, R.S.; , "A MIMO radar system approach to target tracking," Signals, Systems and Computers, 2009 Conference Record of the Forty-Third Asilomar Conference on , vol., no., pp.1186-1190, 1-4 Nov. 2009.

[18] Godrich, H.; Chiriac, V.M.; Haimovich, A.M.; Blum, R.S.; , "Target tracking in MIMO radar systems: Techniques and performance analysis," Radar Conference, 2010 IEEE , vol., no., pp.1111-1116, 10-14 May 2010.

[19] H. Godrich and A. M. Haimovich, "Localization performance of coherent MIMO radar systems subject to phase synchronization errors," Communications, Control and Signal Processing (ISCCSP), 2010 4th International Symposium on , vol., no., pp.1-5, 3-5 March 2010.

[20] H. Godrich, A. M. Haimovich, and R. S. Blum, "A comparative study of target localization in MIMO radar systems," in IEEE Intl. Waveform Diversity and Design Conf., February 2009, pp. 124 - 128.

[21] H. Godrich, A. M. Haimovich, and R. S. Blum, "Target localization accuracy and multiple target localization: Tradeoff in MIMO radars," in Proc. of 42th Asilomar Conf. Signals, Syst. Comput., October 2008, pp. 614 - 618.

[22] H. L. VanTrees, *Detection, Estimation and Modulation Theory: Optimum Array Processing Vol. 4*. New York: Wiley, 2002.

[23] P. Stoica and A. Nehorai, "MUSIC, maximum likelihood, and Cramér-Rao bound," IEEE Trans. Acoust., Speech, & Sig. Proc., vol. 37, pp 720–741, May 1989.

[24] M. Wax and I. Ziskind, "On unique localization of multiple sources by passive sensor arrays ," Acoustics, Speech and Signal Processing, IEEE Transactions on , vol.37, no.7, pp.996-1000, Jul 1989.

7 Interactions/Transitions

7.1 Participation/presentations at meetings, conferences, seminars, etc

- MIMO radar tutorial, 2009 IEEE Radar Conference

- Invited talk, Lehigh University, June 2009

- Invited talk, University of Delaware, Nov. 2011

7.2 Transitions

- Invited talk, AFRL, July 2009

- MIMO radar course, US Army, CERDEC, Sept. 2011 - Oct. 2012.

8 New Discoveries, Inventions, or Patent Disclosures

- 09-046 Location and Speed Estimation in Distributed MIMO Radar with Gaussian Pulse Train Waveforms Carl Georgeson 11/23/2010 Approved

- 09-048 Sidelobe Reduction in Distributed MIMO Radar with Multi-Carrier OFDM Signals Carl Georgeson 11/23/2010 Approved

- 10-019 Algorithms for Target Location and Velocity Tracking in Distributed MIMO Radar Systems Carl Georgeson 11/23/2010 Approved

9 Honors and Awards

Ying Wu Endowed Chair, Oct. 2011.